POSSIBILITIES OF PRODUCTION OF HEAVIEST NUCLEI*

N.V. Antonenko[a], G.G. Adamian[a], A.N. Bezbakh[a]
V.V. Sargsyan[a], T.M. Shneidman[a,b,c], W. Scheid[d]

[a]Joint Institute for Nuclear Research, 141980 Dubna, Russia
[b]State Key Laboratory of Theoretical Physics, Institute of Theoretical Physics
Chinese Academy of Sciences, Beijing 100190, China
[c]Kazan Federal University, Kazan 420008, Russia
[d]Institut für Theoretische Physik der Justus-Liebig-Universität
35392 Giessen, Germany

(Received November 18, 2015)

Impact of nuclear structure on the production of superheavy nuclei in complete fusion reactions is discussed. Possible proton shell closure at $Z = 120$ is considered.

DOI:10.5506/APhysPolBSupp.8.529
PACS numbers: 21.60.Cs, 27.90.+b, 25.70.Jj

1. Introduction

The investigation of transfermium elements expands our knowledge of the single-particle structure, location of the shell closures, and decay modes of heaviest nuclei. The experiments on complete fusion reactions with ^{48}Ca beam and various actinide targets were successfully carried out at FLNR (Dubna), GSI (Darmstadt), and LBNL (Berkeley) [1–7] in order to synthesize superheavy nuclei with $Z = 112$–118.

The further extension of the superheavy region could be reached with complete fusion reactions with projectiles ^{50}Ti and ^{54}Cr, and actinide targets. New isotopes of heaviest nuclei could be produced either in complete fusion reactions with stable and radioactive beams or in the multinucleon transfer reactions. Each way has to be studied to choose the optimal one for certain new nucleus or isotope.

* Presented at the XXII Nuclear Physics Workshop "Marie and Pierre Curie", Kazimierz Dolny, Poland, September 22–27, 2015.

Although the low cross sections for production of superheavy nuclei offer rather restricted nuclear-structure information, in recent years a set of the experimental data on the structure of the heaviest nuclei has been considerably increased. The structure of superheavies crucially influences their evaporation residue cross sections [8].

The systematic of cross sections and half-lives of the SHE obtained in Dubna with ^{48}Ca induced reactions reveals the increasing stability of nuclei approaching the spherical closed shell $N = 184$. No discontinuity is observed when the proton number 114 is crossed at the neutron numbers 172 to 176. As known, the shell at $Z = 114$ disappears in the relativistic and nonrelativistic mean field models [9,10]. The island of stability close to the element $Z = 120$, or 124, or 126 and $N = 184$ was predicted within these models. If these predictions are correct, the survival probability of compound nucleus with $Z \geq 120$ may be higher than that of compound nucleus with $Z = 114$ if the shell closure at $Z \geq 120$ has a stronger influence on the stability of the SHE than the subshell closure at $Z = 114$. Then, there is some hope to synthesize new SHE with $Z \geq 120$ by using the present experimental setup.

2. Trends of survival probabilities

The dinuclear system (DNS) model [11] is successful in describing fusion–evaporation reactions especially related to the production of superheavy nuclei. In the DNS model, the compound nucleus is reached by a diffusion of nucleons from the light nucleus to the heavy one. The evaporation residue cross section is written as

$$\sigma_{xn}(E_{\rm cm}) \;=\; \sigma_{\rm fus}^{\rm eff}(E_{\rm cm}) W_{xn}(E_{\rm cm}, J=0)\,, \tag{1}$$

where the effective fusion cross section

$$\sigma_{\rm fus}^{\rm eff}(E_{\rm cm}) \;=\; \frac{\pi\hbar^2}{\mu E_{\rm cm}} \times \int_0^{\infty}\int_0^{\pi/2}\int_0^{\pi/2} \frac{dJ d\cos\Theta_1 d\cos\Theta_2 \; J e^{-\frac{J^2}{J_m^2(x)}} P_{\rm CN}(E_{\rm cm}, J, \Theta_i)}{1+\exp[2\pi(V_J(R_b,\Theta_i)-E_{\rm cm})/\hbar\omega_J(\Theta_i)]} \tag{2}$$

depends on the probability $P_{\rm CN}$ of complete fusion, which takes into account the competition between complete fusion and quasifission, and capture cross section. In (1), $W_{\rm sur}$ is the survival probability [11]. Here, the collisions of deformed nuclei are taken into account at any orientations. The effective nucleus–nucleus potential

$$V_J(R,\Theta_i) = V_{\rm N}(R,\Theta_i) + V_{\rm C}(R,\Theta_i) + \hbar^2 J(J+1)/(2\Im)$$

is calculated as a sum of nuclear $V_{\rm N}$, Coulomb $V_{\rm C}$ and centrifugal interactions ($\Im$ is the moment of inertia) and approximated near the Coulomb barrier at $R = R_b$ by the inverted harmonic-oscillator potential with the barrier height $V_J(R_b, \Theta_i)$ and frequency $\omega_J(\Theta_i)$. The angular momentum dependence of survival probability is taken into account as in Ref. [8].

Using Eq. (1), one can extract the value of survival probability at zero angular momentum from the experimental cross section $\sigma_{xn}^{\rm exp}(E_{\rm cm})$ as

$$W_{xn}(E_{\rm cm}, J = 0) = \sigma_{xn}^{\rm exp}(E_{\rm cm}) \Big/ \sigma_{\rm fus}^{\rm eff}(E_{\rm cm})\,. \tag{3}$$

With the reduction to the zero angular momentum, the survival probability becomes independent of the projectile–target combination. The fusion probability and, correspondingly, the effective fusion cross section $\sigma_{\rm fus}^{\rm eff}(E_{\rm cm})$ decreases by about 2 orders of magnitude with increasing the charge number of compound nucleus from $Z = 112$ to $Z = 118$ (Fig. 1). The contribution of quasi-fission to the reaction cross section strongly increases with Z due to the increasing Coulomb repulsion in the DNS.

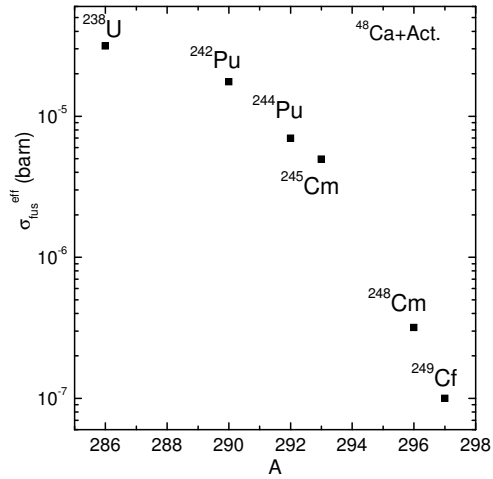

Fig. 1. Effective fusion cross section as a function of mass number of compound nucleus in ^{48}Ca-induced fusion reactions at $E_{\rm cm}$ corresponding to the maximum yields in the $3n$ evaporation channel. Actinide targets are indicated.

In Fig. 2, the extracted values of W_{3n} and W_{4n} increase with Z beyond expected magic proton number $Z = 114$. This indicates an increase of the stability of SHE beyond $Z = 114$. The experimental error bars are the origin of the error bars in the deduced W_{xn}. Since the fission barrier is determined by the shell correction energy, the absolute value of the shell correction energy is expected to increase with Z. The shell correction energy strongly

depends on that how the neutron and proton numbers of the compound nucleus are close to the magic proton and neutron numbers. The found experimental trend of Q_α-values in the α-decay chains also indicates the monotonic increase of the amplitude of the ground state shell correction energy with charge number in the region $Z = 112$–118 [12]. One can expect increasing stability of nuclei approaching the closed neutron $N = 184$ shell. However, in Fig. 2 $W_{3n}(^{296}_{180}116) < W_{3n}(^{297}_{179}118)$. This probably indicates that $Z = 114$ is not a proper proton magic number and the next doubly magic nucleus beyond ^{208}Pb is the nucleus with $Z \geq 120$. The shell closure at $Z \geq 120$ may influence stronger on the stability of the SHE than the sub-shell closure at $Z = 114$. Note that the experimental uncertainties seem to be too small to overcome the trends presented in Fig. 2.

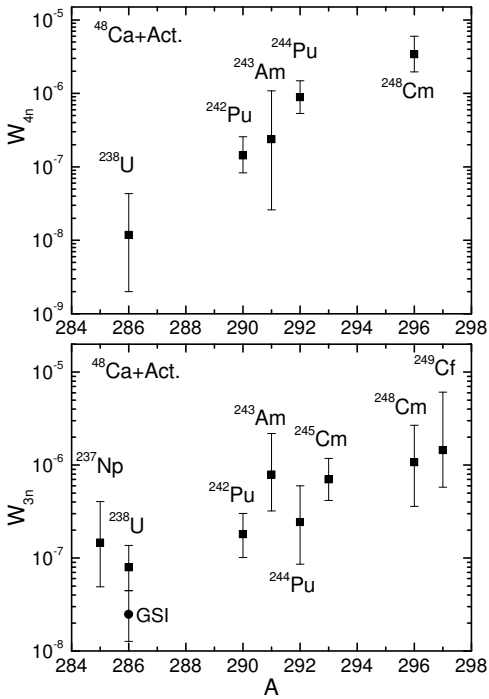

Fig. 2. The survival probabilities of SHE in $3n$-and $4n$-channels, extracted from the experimental $\sigma_{xn}^{\rm exp}$ [1], as functions of mass number of the compound nucleus. For the reaction ^{48}Ca+^{238}U, the experimental $\sigma_{3n}^{\rm exp}$ from Ref. [12] is used as well.

3. Properties of superheavy nuclei

The microscopic–macroscopic approaches provide a powerful tool for systematic calculations and predictions which are important for the experiments planned. One of these approaches is based on the two-center shell model

(TCSM) [13]. Calculating the quadrupole and hexadecapole moments, one can find the relationship between the deformation parameters used in the TCSM, and the parameters of quadrupole β_2 and hexadecapole β_4 deformation used in the models of Refs. [14, 15]. The ground state of the nucleus is resulted from the calculation of the potential energy surface as a function of deformation parameters [16]. The ground state of ^{248}Fm is found at $\beta_2 = 0.26$ and $\beta_4 = 0.03$. For comparison, in Ref. [15] $\beta_2 = 0.235$ and $\beta_4 = 0.049$ for this nucleus. The ground state of ^{270}Hs is found at $\beta_2 = 0.25$ and $\beta_4 = -0.03$. In Ref. [15], $\beta_2 = 0.231$ and $\beta_4 = -0.086$ are predicted for this nucleus. While in ^{268,269,270,271}Hs, the microscopic corrections in Ref. [15] are -5.95, -6.38, -6.54, and -6.64 MeV, respectively, we get -5.75, -6.37, -6.1, and -6.0 MeV. So, the performed modification of the TCSM for nuclear structure calculations seems to be well confident.

As seen in Fig. 3, the calculated Q_α are in a good, within 0.3 MeV, agreement with the available experimental data. The shell effects at $Z = 114$ and $N = 172$–176 provide rather weak dependence of Q_α on N. The strong role of the shell at $N = 184$ is reflected in the well pronounced minimum of Q_α. For comparison, the Q_α-values predicted in Ref. [15] are shown in

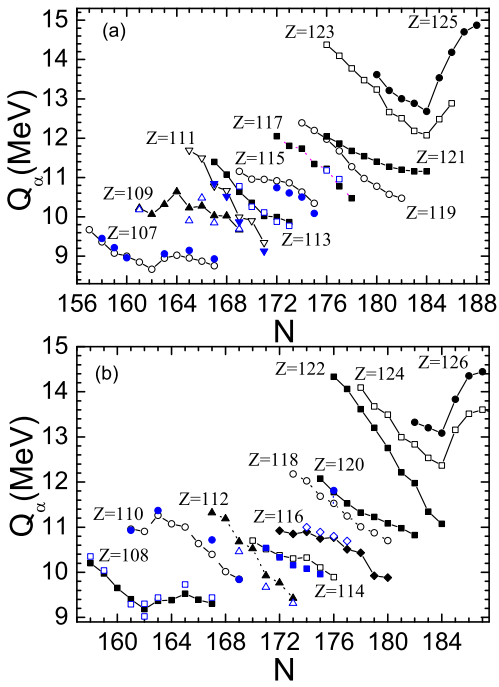

Fig. 3. Calculated α-decay energies (symbols connected by lines) are compared with available experimental data (symbols) [1, 2, 4, 6] for nuclei with $Z \geq 107$.

Fig. 4. As in our case, the dependence of Q_α on N becomes weaker at $N = 172$–176 with the data of Ref. [15]. The small role of $N = 184$ and $Z = 120$–126 is seen in Fig. 4. The phenomenological model [17] results in no shell effects at $N = 162$ and at $N = 172$–176. However, as in our calculations, there is a strong evidence of the shell closure at $N = 184$. The details of our calculations are presented in Ref. [18]. The paring was treated with the BCS approximation. For odd-masses, the blocking effect was effectively taken into account [18].

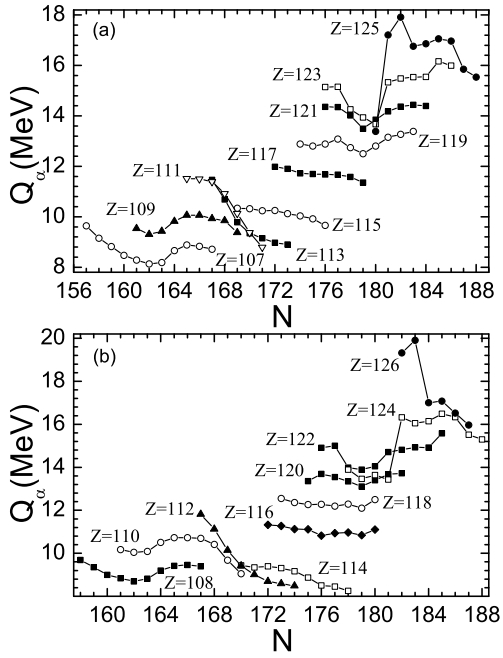

Fig. 4. α-decay energies (symblos connected by lines) calculated with the macroscopic–microscopic model [15] for nuclei with $Z \geq 107$.

The value of survival probability strongly depends on $B_f - B_n$, the difference between the height B_f of the fission barrier and the neutron separation energy B_n. The value of B_f is assumed to be mainly determined by the amplitude of the shell correction in the ground state for nuclei with $Z \geq 106$. This assumption could cause the main uncertainty in the definition of survival probability. At fixed charge number, the predicted values of B_n steadily decrease in the region of $N \geq 170$ with increasing N. The values of B_n predicted with different models vary within 0.5 MeV and the shell effects or B_f cause the difference in the dependencies of $B_f - B_n$ on N. As seen in Fig. 5, our macroscopic–microscopic approach provides stronger shell effects at $Z = 120$–126 than at $Z = 114$. Since for nuclei with $Z = 120$–126 the

values of Q_α are minimal at $Z = 120$ (Fig. 3) where the fission barriers are rather high, the nuclei with $Z = 120$ and $N = 180$–184 are expected to be the most stable nuclei beyond those with $Z = 114$ and $N = 176$–178. The shell closure at $Z = 120$ is expected to be in accordance with the relativistic mean-field model as well.

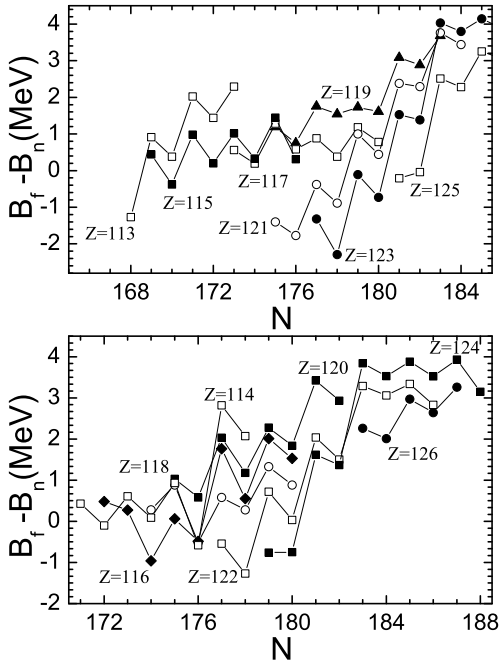

Fig. 5. The isotopic dependence of the value of $B_f - B_n$ with the TCSM data. The fission barrier B_f is assumed to be an absolute value of the shell correction in the ground state of the nucleus. The results for the isotopes related to the indicated even charge number Z are shown by symbols connected by lines.

In Fig. 6, the energies of two-quasiparticle states are presented for the nuclei of α decay chains of $^{296,298}120$. While for nuclei with $Z \leq 118$ the first two-quasiproton states have energies smaller than 1.2 MeV, in $^{296,298}120$ the energies of the first two-quasiproton state are at about 1.9 MeV. This indicates the larger gap in the proton single-particle spectrum. So, the shell effects become stronger beyond $Z = 114$.

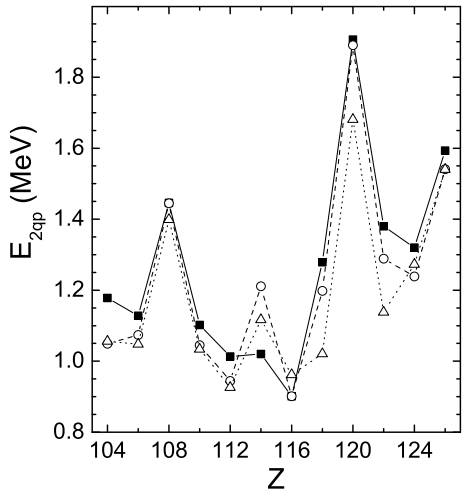

Fig. 6. Calculated energies of the lowest two-quasiproton states in the indicated nuclei of α-decay chains of $^{308}126$ (solid squares), $^{310}126$ (open circles), and $^{312}126$ (open triangles) nuclei.

4. Expected cross sections

The available experimental $\sigma_{\rm ER}$ for $Z \leq 118$ are well described [11] with our approach. The evaporation residue cross sections at the maxima of (2–4)n excitation functions and corresponding optimal excitation energies $E^*_{\rm CN}$ calculated with the mass tables of Ref. [15] are presented in Fig. 7 for

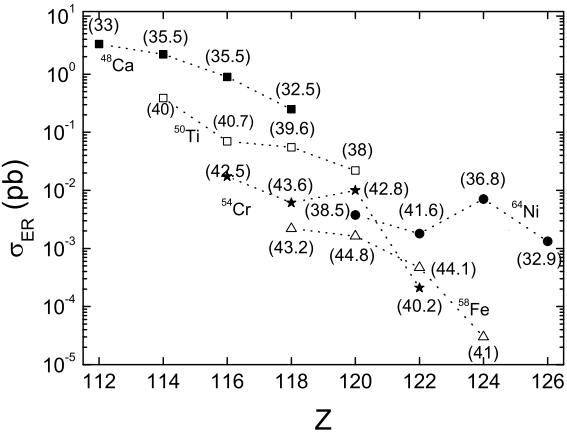

Fig. 7. The evaporation residue cross sections in the maxima of excitation functions *versus* charge number Z for the reactions ^{48}Ca, ^{50}Ti, ^{54}Cr, ^{58}Fe, ^{64}Ni+ ^{238}U, ^{244}Pu, ^{248}Cm, ^{249}Cf. The predicted properties of superheavy nuclei from Ref. [18] are used. The excitation energies of compound nuclei are given in brackets.

the reactions ^{50}Ti, ^{54}Cr, ^{58}Fe, ^{64}Ni + ^{238}U, ^{244}Pu, ^{248}Cm, ^{249}Cf. The values of $\sigma_{\rm ER}$ decrease by about two–three orders of magnitude with increasing the charge number of the target from 92 to 98. Only the projectiles ^{50}Ti, ^{54}Cr result in the production cross section of $Z = 114$, 116, 118 on the level of the present experimental possibilities. The stronger shell effect revealed here for nuclei with $Z > 118$ result in larger survival probabilities and larger values of $\sigma_{\rm ER}$.

In Fig. 8, the dependence of $\sigma_{\rm ER}$ on the mass number of the target nucleus is shown. As in Ref. [19], the isotopic dependence of $\sigma_{\rm ER}$ is rather weak in the treated interval of A. There is certain interval of mass number of target nucleus where the product $P_{\rm CN}W_{\rm sur}$ weakly changes.

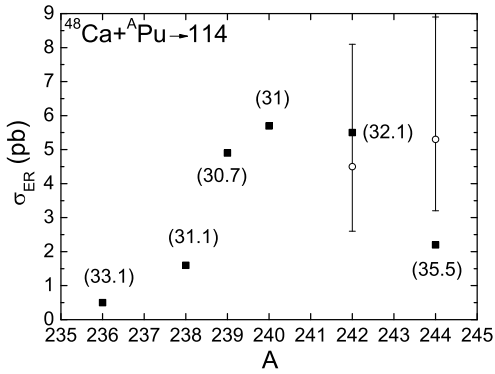

Fig. 8. The evaporation residue cross sections in the maxima of excitation functions of the reactions ^{48}Ca+^{A}Pu *versus* A. The excitation energies of compound nuclei are given in brackets.

5. Summary

The calculations performed with the modified TCSM reveal quite strong shell effects at $Z = 120$–126. So, our macroscopic–microscopic treatment qualitatively leads to the results close to those in the mean-field treatments. The strong shell effect is at $N = 184$. If our predictions of the structure of heaviest nuclei are correct, than one can expect the production of evaporation residues 120 in the reactions ^{50}Ti+^{249}Cf and ^{54}Cr+^{248}Cm with the cross sections 23 and 10 fb. The $Z = 120$ nuclei with $N = 178$–182 are expected to have Q_α about 11 MeV and life time of about 1 s. These Q_α are in a fair agreement with Ref. [17] and about 2 MeV smaller than in Refs. [14, 15]. The experimental detection of Q_α for at least one isotope of $Z = 120$ nucleus would help us to set the proper shell model for $Z > 118$. Note that the definition of maxima of the excitation functions provides the good test for the predictions of the models as well.

T.M.S. acknowledges the support from the CAS Fellowship for the Young International Scientists (2013Y1JA0003) and Russian Government Subsidy Program of the Competitive Growth of Kazan Federal University. This work was supported in part by RFBR. The Polish–JINR (Dubna) Cooperation Programmes are gratefully acknowledged.

REFERENCES

[1] Yu.Ts. Oganessian, *J. Phys. G* **34**, R165 (2007).
[2] Yu.Ts. Oganessian *et al.*, *Phys. Rev. Lett.* **104**, 142502 (2010).
[3] Yu.Ts. Oganessian *et al.*, *Phys. Rev. C* **87**, 014302 (2013).
[4] S. Hofmann *et al.*, *Eur. Phys. J. A* **32**, 251 (2007).
[5] W. Loveland *et al.*, *Phys. Rev. C* **66**, 044617 (2002); K.E. Gregorich *et al.*, *Phys. Rev. C* **72**, 014605 (2005).
[6] L. Stavsetra *et al.*, *Phys. Rev. Lett.* **103**, 132502 (2009).
[7] D. Rudolph *et al.*, *Phys. Rev. Lett.* **111**, 112502 (2013).
[8] G.G. Adamian, N.V. Antonenko, W. Scheid, *Eur. Phys. J. A* **41**, 235 (2009).
[9] P.G. Reinhard, *Rep. Prog. Phys.* **52**, 439 (1989); P. Ring, *Prog. Part. Nucl. Phys.* **37**, 193 (1996); M. Bender, P.H. Heenen, P.G. Reinhard, *Rev. Mod. Phys.* **75**, 121 (2003).
[10] J. Meng *et al.*, *Prog. Part. Nucl. Phys.* **57**, 470 (2006).
[11] G.G. Adamian, N.V. Antonenko, W. Scheid, *Nucl. Phys. A* **678**, 24 (2000); *Phys. Rev. C* **68**, 034601 (2003); **69**, 014607 (2004); **69**, 044601 (2004); **72**, 064617 (2005); A.S. Zubov *et al.*, *Phys. Rev. C* **68**, 014616 (2003); **71**, 034603 (2005).
[12] S. Hofmann *et al.*, *Eur. Phys. J. A* **32**, 251 (2007).
[13] J. Maruhn, W. Greiner, *Z. Physik* **251**, 431 (1972).
[14] I. Muntian, Z. Patyk, A. Sobiczewski, *Acta Phys. Pol. B* **32**, 691 (2001); *Acta Phys. Pol. B* **34**, 2141 (2003); I. Muntian, S. Hofmann, Z. Patyk, A. Sobiczewski, *Acta Phys. Pol. B* **34**, 2073 (2003); *Phys. At. Nucl.* **66**, 1015 (2003); A. Parkhomenko, I. Muntian, Z. Patyk, A. Sobiczewski, *Acta Phys. Pol. B* **34**, 2153 (2003); A. Parkhomenko, A. Sobiczewski, *Acta Phys. Pol. B* **36**, 3095 (2005).
[15] P. Möller *et al.*, *At. Data Nucl. Data Tables* **59**, 185 (1995).
[16] G.G. Adamian, N.V. Antonenko, W. Scheid, *Phys. Rev. C* **81**, 024320 (2010); G.G. Adamian, N.V. Antonenko, S.N. Kuklin, W. Scheid, *Phys. Rev. C* **82**, 054304 (2010).
[17] S. Liran, A. Marinov, N. Zeldes, *Phys. Rev. C* **62**, 047301 (2000).
[18] A.N. Kuzmina, G.G. Adamian, N.V. Antonenko, W. Scheid, *Phys. Rev. C* **85**, 014319 (2012).
[19] G.G. Adamian, N.V. Antonenko, W. Scheid, *Phys. Rev. C* **69**, 011601(R) (2004); **69**, 014607 (2004); **69**, 044601 (2004).